Received: 17 January 2018 | Revised: 11 April 2018 | Accepted: 17 April 2018

DOI: 10.1002/bit.26717

ARTICLE

WILEY BIOTECHNOLOGY BIOENGINEERING

High-efficiency affinity precipitation of multiple industrial mAbs and Fc-fusion proteins from cell culture harvests using Z-ELP-E2 nanocages

Andrew R. Swartz[1] | Xuankuo Xu[2] | Steven J. Traylor[2] | Zheng Jian Li[2] | Wilfred Chen[1]

[1]Department of Chemical and Biomolecular Engineering, University of Delaware, Newark, Delaware

[2]Biologics Process Development, Bristol Myers Squibb, Devens, Massachusetts

Correspondence
Wilfred Chen, Chemical and Biomolecular Engineering, University of Delaware, Colburn Laboratory 150 Academy St., Newark, DE 19716.
Email: wilfred@udel.edu

Funding information
Division of Chemical, Bioengineering, Environmental, and Transport Systems, Grant/Award Number: CBET1403724

Abstract

Affinity precipitation using Z-elastin-like polypeptide-functionalized E2 protein nanocages has been shown to be a promising alternative to Protein A chromatography for monoclonal antibody (mAb) purification. We have previously described a high-yielding, affinity precipitation process capable of rapidly capturing mAbs from cell culture through spontaneous, multivalent crosslinking into large aggregates. To challenge the capabilities of this technology, nanocage affinity precipitation was investigated using four industrial mAbs (mAbs A–D) and one Fc fusion protein (Fc A) with diverse molecular properties. A molar binding ratio of 3:1 Z:mAb was sufficient to precipitate >95% mAb in solution for all molecules evaluated at ambient temperature without added salt. The effect of solution pH on aggregation kinetics was studied using a simplified two-step model to investigate the protein interactions that occur during mAb–nanocage crosslinking and to determine the optimal solution pH for precipitation. After centrifugation, the pelleted mAb–nanocage complex remained insoluble and was capable of being washed at pH ≥ 5 and eluted with at pH < 4 with >90% mAb recovery for all molecules. The four mAbs and one Fc fusion were purified from cell culture using optimal process conditions, and >94% yield and >97% monomer content were obtained. mAb A–D purification resulted in a 99.9% reduction in host cell protein and >99.99% reduction in DNA from the cell culture fluids. Nanocage affinity precipitation was equivalent to or exceeded expected Protein A chromatography performance. This study highlights the benefits of nanoparticle crosslinking for enhanced affinity capture and presents a robust platform that can be applied to any target mAb or Fc-containing proteins with minimal optimization of process parameters.

KEYWORDS
affinity precipitation, bioseparation, elastin-like polypeptide, monoclonal antibody, nanoparticle

1 | INTRODUCTION

Advancements in the upstream production of therapeutic monoclonal antibodies (mAbs) have challenged current platform downstream purification technologies (Shukla & Thömmes, 2010). Protein A affinity chromatography is commonly used as the primary antibody capture step because of the high selectivity of the Protein A ligand to the Fc region present on human immunoglobulin G (IgG; Hober, Nord, &

 © 2018 Wiley Periodicals, Inc.

Linhult, 2007). However, economic, throughput, and scale-up limitations make Protein A affinity chromatography a potential bottleneck in the overall mAb production process (Low, O'Leary, & Pujar, 2007). Affinity precipitation has been investigated as a more cost-effective and scalable alternative (Hillbrig & Freitag, 2003; Thommes & Etzel, 2007), but the technique has not been widely implemented in industry because of low mAb yields, coprecipitation of contaminants, and use of harsh chemicals or solution conditions (Gagnon, 2012).

Affinity precipitation using a stimuli-responsive, recombinant elastin-like polypeptide (ELP) genetically fused to an IgG binding domain called the Z-domain (Z-ELP) has been shown to be a promising scaffold for selective IgG capture (Madan, Chaudhary, Cramer, & Chen, 2013; Sheth et al., 2014; Sheth, Madan, Chen, & Cramer, 2013). However, the elevated salt and temperature required for ELP precipitation resulted in increased mAb aggregation and decreased operational efficiency. We recently designed an enhanced antibody capture scaffold by covalently conjugating Z-ELP to a 25 nm self-assembled, 60-mer E2 protein nanocage (Z-ELP-E2) using sortase A ligation (Swartz, Sun, & Chen, 2017). Multivalent IgG binding triggered spontaneous crosslinking into large IgG-Z-ELP-E2 aggregates that allowed for easy precipitation and separation, and the recovered IgG-Z-ELP-E2 complex remained insoluble until dissociation with a low-pH elution.

We performed high-throughput process optimization using a model industrial mAb, and developed a simple, one-step antibody affinity capture and precipitation platform for mAb purification from Chinese hamster ovary (CHO) cell culture fluids with equivalent yields and impurity clearance compared with Protein A chromatography (Swartz, Xu, Traylor, Li, & Chen, 2018). On mixing at a 3:1 Z-domain:mAb molar ratio, >95% mAb was precipitated within minutes at ambient temperature without added salt due to extensive nanocage crosslinking. High mAb recovery was obtained after washing at pH ≥ 5, followed by elution at pH < 4, and the purification process was repeated over several cycles using the same regenerated nanocage with a similar process efficiency.

For a more robust examination of this technology as an alternative to Protein A chromatography, the general utility of the approach was further evaluated using four industrial mAbs and one Fc fusion protein with diverse attributes, such as IgG subclass, isoelectric point (pI), and culture harvest titers (Table 1). Key process conditions, such as the molar binding ratio, aggregation time, and elution pH, were tested using purified mAb and nanocage stocks. A two-step kinetic model was applied to examine the dependence of the solution pH on aggregation rates. Operational conditions were identified to maximize the mAb yield and monomer content for each target molecule, while minimizing operation time (Table 2). Finally, the mAb yield, monomer content, and host cell protein (HCP) and DNA clearance from clarified CHO cell cultures were compared with typical Protein A chromatography (Fahrner et al., 2001).

TABLE 1 Molecular properties and concentrations of the five molecules used in the study

No.	Molecule name	IgG subclass	MW (kDa)	pI	Culture titer (mg/ml)	Purified stock (mg/ml)
1	mAb A	IgG4	147	8.2	6.1	66.8
2	mAb B	IgG4	155	6.8	3.1	63.0
3	mAb C	IgG1	150	8.3	1.8	61.2
4	mAb D	IgG1	152	9.1	5.1	45.6
5	Fc A	Fc-IgG1	79	5.8	2.8	40.8

Note. IgG, immunoglobulin G; mAb, monoclonal antibody; MW, molecular weight; pI, isoelectric point.

2 | MATERIALS AND METHODS

2.1 | Materials

Escherichia coli strain BLR(DE3) containing pET24(a) vectors encoding for Z-ELP[KV_8F-40]-LPETG, *E. coli* strain BL21(DE3) containing a pET11(a) vector encoding for GGG-E2(158), and another BL21(DE3) strain containing a pMR5 vector encoding for SrtA were constructed and described previously (Swartz et al., 2017). Purified and clarified cell culture mAb and Fc-fusion samples were provided by Bristol-Myers Squibb (BMS; New York City, NY). Bacto tryptone and yeast extract were purchased from BD Biosciences (Franklin Lakes, NJ). Kanamycin, ampicillin, bovine serum albumen, isopropyl-β-D-thiogalactoside, and 96-well 200 µl conical PCR plates were purchased from Thermo Fisher Scientific (Pittsburgh, PA). A human polyclonal IgG, sodium hydroxide, sodium phosphate, citric acid, tris base, ammonium sulfate, sodium chloride, L-arginine, and Polysorbate-80 (PS-80) were purchased from Sigma-Aldrich (St. Louis, MO). 0.8/0.2 µm Supor Acrodisc syringe filters were purchased from Pall (Port Washington, NY). 100 kDa Sartorius Vivaspin 20 spin columns were purchased from Sartorius (Göttingen, Germany). 96-well half-area UV-transparent plates were purchased from Corning (Corning, NY). An Acquity UPLC BEH size exclusion chromatography (SEC) column (200 Å, 1.7 µm, 4.6 × 300 mm) was purchased from Waters (Milford, MA).

2.2 | Experimental methods

2.2.1 | Z-ELP-E2 nanocage production

Z-ELP[KV_8F-40]-LPETG, a modified GGG-E2 from *Bacillus stearothermophilus*, and sortase A from *Staphylococcus aureus* were expressed in *E. coli* and Z-ELP was conjugated to E2 using the previously described procedures (Swartz et al., 2018). Briefly, Z-ELP purified by inverse transition cycling (ITC; Meyer & Chilkoti, 1999), E2 partially purified by 70°C heating, and sortase A soluble lysate were mixed in a reaction buffer for 8 hr at 23°C and the ligation product was purified by ITC into phosphate-buffered saline (PBS; 20 mM sodium phosphate, 150 mM sodium chloride, pH 7.2). 100 kDa Sartorius Vivaspin 20 spin columns were used to remove excess Z-ELP and two more ITC cycles were used to further concentrate the purified Z-ELP-E2 stock. Z-ELP ligation density on E2 was determined by densitometry analysis of an SDS-PAGE gel and Z-ELP concentration was measured using absorbance at 280 nm and an experimentally determined extinction coefficient.

TABLE 2 Affinity precipitation conditions used for purification of the molecules from cell culture

Molecule name	[Z]:[mAb] binding ratio	Precipitation pH	Wash 1 buffer	Wash 2 buffer	Wash 3 buffer	Elution buffer	Nanocage precipitation (AS)
mAb A	3:1	7	PBS, pH 7.2	Salt, excipient, PS-80, pH 9.0	Citrate, pH 5.0	Citrate, pH 3.75	0.2 M
mAb B	3:1	5	Citrate, pH 5.0	Salt, excipient, PS-80, pH 9.0	Citrate, pH 5.0	Citrate, pH 3.75	0.2 M
mAb C	3:1	7	PBS, pH 7.2	Salt, excipient, PS-80, pH 9.0	Citrate, pH 5.0	Citrate, pH 3.50	0.3 M
mAb D	3:1	7	PBS, pH 7.2	Salt, excipient, PS-80, pH 9.0	Citrate, pH 5.0	Citrate, pH 3.50	0.2 M
Fc A	3:1	5	Citrate, pH 5.0	Citrate, excipient, pH 7.0	Citrate, pH 5.0	Citrate, pH 3.50	0.3 M

Note. AS, ammonium sulfate; mAb, monoclonal antibody; PBS, phosphate-buffered saline; PS-80, Polysorbate-80.

2.2.2 | High-throughput affinity precipitation experiments

Previous work used an mAb designated "mAb C" in the current investigation (Swartz et al., 2018). All experiments using mAb C were repeated using the indicated procedures below. High-throughput affinity precipitation experiments were performed using 200 µl 96-well conical PCR plates at 23°C with previously purified mAbs and Z-ELP-E2 nanocage stocks. For all centrifugation steps, the plate was spun at 1,500 *g* for 30 min at 23°C. Supernatant samples were collected using a multichannel pipette and transferred into a UV-transparent 96-well plate for the measurement of absorbance at 280 nm on a Tecan Infinite M1000 plate reader (Männedorf, Switzerland). mAb concentrations were determined using the theoretical extinction coefficient for each molecule. The supernatants were assumed to contain only mAb based on previous results (Swartz et al., 2018). For binding ratio experiments, 20 µM mAb samples were mixed with 20–100 µM Z-ELP-E2 (1:1 to 5:1 Z-domain:mAb molar ratio) in PBS for 1 hr before centrifugation for mAbs A–D. Fc A was mixed for 3 hr before centrifugation. The supernatant was collected and the mAb precipitation yield was calculated (Yield =1 – $[mAb_{supe}]/[mAb_{initial}]$). For precipitation kinetic experiments, 10 µM mAb was mixed with 30 µM Z-ELP-E2 in PBS for various incubation times ranging from 2 min to 3 hr before centrifugation. The supernatant was collected and mAb precipitation yield was calculated. For mAb elution experiments, 10 µM mAb was mixed with 30 µM Z-ELP-E2 in PBS for 1–3 hr before centrifugation. The precipitation supernatant was removed and the pellet was suspended in a 25 mM sodium citrate pH 5.0 wash buffer by aspirating and dispensing using a pipette. After another spin, the wash supernatant was removed and the pellet was suspended in 50 mM sodium citrate buffers with a pH ranging from 3.50 to 4.50 and mixed for 30 min. Samples were adjusted to 0.4 M ammonium sulfate using a 3 M stock before centrifuging again. The supernatant was collected and mAb elution yield was calculated (Yield = 1 – $[mAb_{elution}]/[mAb_{initial}]$). All experimental conditions were performed in triplicate and 95% confidence intervals of the mean value were reported.

2.2.3 | Aggregation kinetic measurements

Solutions were prepared ranging from pH 5 to 9 using the indicated buffers and were adjusted to 150 mM total ionic strength by the addition of sodium chloride (Supporting Information Table SI). Samples were prepared with 1 µM mAb and 3 µM Z-ELP-E2 in a target buffer in a 96-well UV transparent plate and immediately placed in a Synergy plate reader from BioTek (Winooski, VT) for kinetic measurement of absorbance at 350 nm for various times ranging from 5 to 300 min. A human polyclonal antibody used in the previous work was included in this investigation (Swartz et al., 2017). Data were collected until peak absorbance as some samples settled out of solution over time, causing a decrease in signal. The Finke–Watzky two-step model of pseudoelementary nucleation (Equation 1) and autocatalytic growth (Equation 2) was applied as follows (Morris, Watzky, Agar, & Finke, 2008):

$$A \xrightarrow{k_1} B \tag{1}$$

$$A + B \xrightarrow{k_2} 2B \tag{2}$$

where A represents the monomeric nanocage with bound mAbs, B represents the polymeric mAb-nanocage aggregate, and k_1 and k_2 represent the average rate constants for nucleation and autocatalytic growth. Rate constants were assumed to be independent of aggregate size or morphology. The overall reaction rate for A is expressed as follows:

$$\frac{d[A]}{dt} = -k_1[A] - k_2[A][B] \tag{3}$$

where [A] and [B] represent the concentrations of A and B, respectively, at time *t*. It was assumed that there are no aggregates initially $[B]_0 = 0$, such that the $[B] = [A]_0 - [A]$ at all times. On integration of the rate law and further simplification, the expression for the increase in B over time was obtained as follows:

$$[B] = [A]_0 - \frac{\frac{k_1}{k_2} + [A]_0}{1 + \frac{k_1}{k_2[A]_0} e^{(k_1 + k_2[A]_0)t}}. \tag{4}$$

The values of k_1 and k_2 were fit by nonlinear regression in Minitab 17 using normalized absorbance curves representing

aggregate (B) formation over time and the 95% confidence interval of the fit was reported. The time at inflection (t_{max}) of the aggregation curve (maximum aggregation rate) was calculated by setting the second derivative of [B] to zero as follows (Bentea, Watzky, & Finke, 2017):

$$t_{max} = \frac{\ln\left(\frac{k_2 A_0}{k_1}\right)}{k_1 + k_2 A_0}. \quad (5)$$

2.2.4 | mAb culture affinity precipitation

All purification steps were performed at ambient temperature (23°C) using optimized process conditions reported in Table 2. For Fc A and mAb B, the culture was titrated to pH 5.0 using 1 M citric acid before adding the nanocage. For the other molecules, no titration was performed and precipitation was performed directly in cell culture (pH 7.0–7.5). Purified nanocage stock was mixed with mAb culture at a 3:1 Z:mAb molar ratio for 10 min and the mAb–nanocage complex was pelleted by centrifugation. The pellet was washed with a series of three wash buffers before elution by resuspending in threefold less volume 50 mM sodium citrate pH 3.50 for mAb C, mAb D, and Fc A or pH 3.75 for mAb A and mAb B for 60 min. The nanocage was precipitated with 0.2–0.3 M ammonium sulfate and the elution supernatants were titrated to pH 5.5 using 2 M tris pH 11 and assayed for mAb concentration, monomer content, and impurity content. The pelleted nanocage was regenerated in 50 mM sodium citrate pH 3.0 and recycled back into PBS pH 7.2 using ITC. The nanocage was filtered through a 0.8/0.2 µm Supor syringe filter before use in a subsequent purification cycle. The affinity precipitation process was repeated for three cycles for mAb C, D, and Fc A and one cycle for mAb A and B.

2.2.5 | Analytical SEC

mAb stability was monitored by SEC. Samples were diluted to 1 mg/ml mAb, added to a low-volume UPLC vial (Waters), and placed in a temperature-controlled autoinjector set at 4°C in a Waters Acquity UPLC system. A mobile phase of 200 mM potassium phosphate and 150 mM sodium chloride, pH 6.8, was used at a flow rate of 0.4 ml/min. Three injections of 10 µl were performed and the column effluent was monitored at 280 nm. Peak areas were analyzed by Empower Software (Waters).

2.2.6 | Analytical impurity content

CHO cell HCP concentration was determined using an ELISA kit from Cygnus Technologies. CHO cell DNA concentration was determined using an in-house quantitative polymerase chain reaction (qPCR) assay developed at BMS. Details of these assays have been discussed previously (Sheth et al., 2014).

3 | RESULTS AND DISCUSSION

3.1 | Impact of Z-domain-target binding ratio on precipitation yield

The goal of this study was to demonstrate the utility of the Z-ELP-E2 nanocage for the affinity precipitation of multiple mAbs and Fc-fusion proteins with different molecular properties (Table 1). Earlier results using a mAb designated "mAb C" from BMS demonstrated that a 3:1 Z-domain:mAb molar ratio was optimal for precipitation at ambient temperature without any addition of salt (Swartz et al., 2018). To investigate whether this was true for other mAbs or Fc-fusion proteins, Z-ELP-E2 nanocages were mixed with the purified target proteins at molar binding ratios ranging from 1:1 to 5:1 in PBS at 23°C (Figure 1a). Again, a 3:1 binding ratio was sufficient to precipitate approximately 95% mAb in the mixture for all targets tested, suggesting that this was likely the optimal ratio to trigger both efficient nanocage crosslinking and ELP aggregation for purification. The ratio was slightly higher than the expected Z:IgG stoichiometry of 2:1 (Jendeberg et al., 1995), likely due to steric limitations on Z-domain flexibility or accessibility of IgG-binding sites. These results confirmed the suitability of using Z-ELP-E2 nanocages to capture different Fc-containing proteins with similar efficiencies. Although a 4:1 binding ratio exhibited a similarly high precipitation yield,

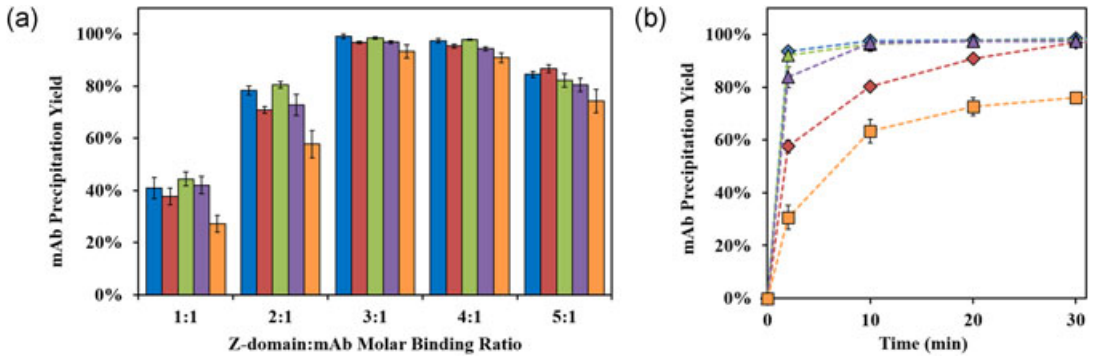

FIGURE 1 mAb binding and precipitation yield. (a) Effect of the Z:mAb binding ratio on the mAb precipitation yield in PBS at 23°C for mAb A (blue), mAb B (red), mAb C (green), mAb D (purple), and Fc A (orange). (b) Effect of mixing time on mAb precipitation yield with 3:1 Z:mAb in PBS at 23°C for mAb A (blue diamond), mAb B (red diamond), mAb C (green triangle), mAb D (purple triangle), and Fc A (orange square). mAb, monoclonal antibody; PBS, phosphate-buffered saline [Color figure can be viewed at wileyonlinelibrary.com]

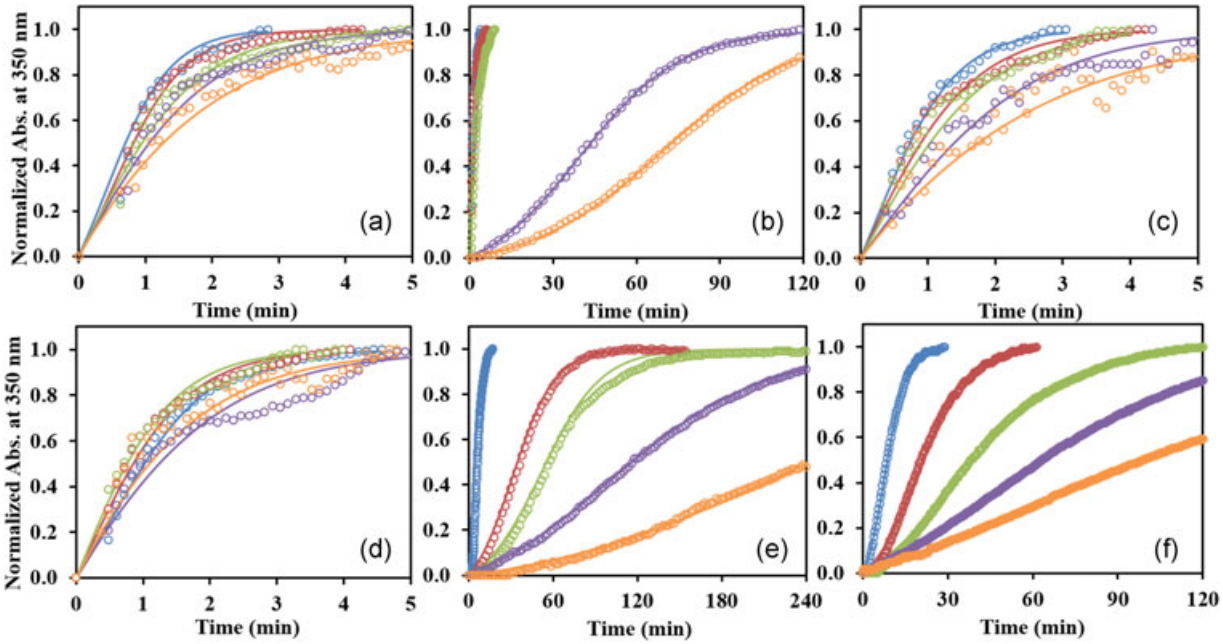

FIGURE 2 Effect of solution pH on aggregation kinetics at 3:1 Z:mAb molar binding ratio for mAb A (a), mAb B (b), mAb C (c), mAb D (d), Fc A (e), and polyclonal antibody (f). Normalized absorbance data (open circle) and F–W model fit (solid line) shown at solution pH 5 (blue), pH 6 (red), pH 7 (green), pH 8 (purple), and pH 9 (orange). mAb, monoclonal antibody [Color figure can be viewed at wileyonlinelibrary.com]

increasing the binding ratio further to 5:1 decreased the yield to less than 80%. These observations are consistent with the molar binding ratio used in other affinity precipitation systems. For the purification of multimeric dehydrogenase enzymes using a bivalent affinity ligand, the optimal precipitation yield occurred at a ligand:protein ratio close to the expected interaction stoichiometry. In addition, excess ligand resulted in lower yields due to the saturation of binding sites on the target protein and reduced crosslinking efficiency (Flygare, Griffin, Larsson, & Mosbach, 1983).

3.2 | Effect of solution pH on aggregation kinetics

The rapid capture and precipitation of mAb C was previously demonstrated to occur within a few min on mixing with the nanocages (Swartz et al., 2018). However, the binding and crosslinking kinetics appeared to differ significantly among the five target proteins in the current study. Samples containing either purified mAb A, C, or D turned cloudy within seconds on mixing with nanocages at a 3:1 Z:mAb molar ratio. In contrast, mAb B and Fc A gradually increased in turbidity over several minutes to hours. To evaluate how the crosslinking kinetics can impact target precipitation and recovery, samples were mixed with nanocages at the same 3:1 Z:mAb binding ratio from 2 min to 3 hr before pelleting the complex (Figure 1b). The nanocage precipitated greater than 90% of mAb A, C, and D from the mixture within 10 min, but required 30 min for mAb B and 3 hr for Fc A to obtain similar yields. The IgG subclass appeared to have no impact on aggregation kinetics because mAbs from both IgG1 (mAb A) and IgG4 (mAb C and D) groups precipitated rapidly. The variable kinetics may be due to differences in the mAb or Fc protein net charge at neutral pH. In PBS at pH 7.2, Fc A (pI = 5.8) and mAb B (pI = 6.8) are both anionic, with a pI value less than the buffer pH, whereas the other mAbs with fast kinetics have pI values greater than eight (Table 1).

To quantify the dependence of solution pH on aggregation kinetics, the Finke–Watzky (F–W) model of nucleation (Equation 1) and growth (Equation 2) was selected to fit aggregation curves over time. This model has been applied to numerous systems to characterize aggregation events (Morris et al., 2008; Watzky, Morris, Ross, & Finke, 2008) and allows for simple quantification of average rate constants by fitting experimental data to the integrated rate law (Equation 4). The F–W model was chosen because it appropriately depicts the previously hypothesized aggregation mechanism of an initial multivalent binding step between two Z-domains from different nanocages and one mAb, followed by autocatalytic crosslinking into large, insoluble particles (Swartz et al., 2017).

The aggregation curves for mAb B, Fc A, and a human polyclonal IgG displayed a strong dependence on solution pH (Figures 2b, 2e, and 2f), whereas mAbs A, C, and D demonstrated fast kinetics with minimal pH dependence in the tested range of pH 5–9 (Figures 2a, 2c, and 2d). The absorbance data were fit to the F–W model and the k_1 and k_2 rate constants were evaluated for each solution condition and molecule (Figure 3). mAb B exhibited fast aggregation at pH 5–7, but a shift occurred between pH 7 and 8 such that both rate constants decreased by an order of magnitude (Figure 3b). In addition, the ratio of the rate constants also differed significantly between the two kinetic regimes. At low pH, the nucleation (k_1) and crosslinking ($k_2{*}A_0$) rate constants were similar, but at pH 8–9, nucleation was the rate-limiting step ($k_1 \ll k_2{*}A_0$). Fc A had very slow kinetics at pH ≥ 7, requiring >60 min to reach the maximum aggregation rate (t_{max}; Supporting Information Figure S1). However,

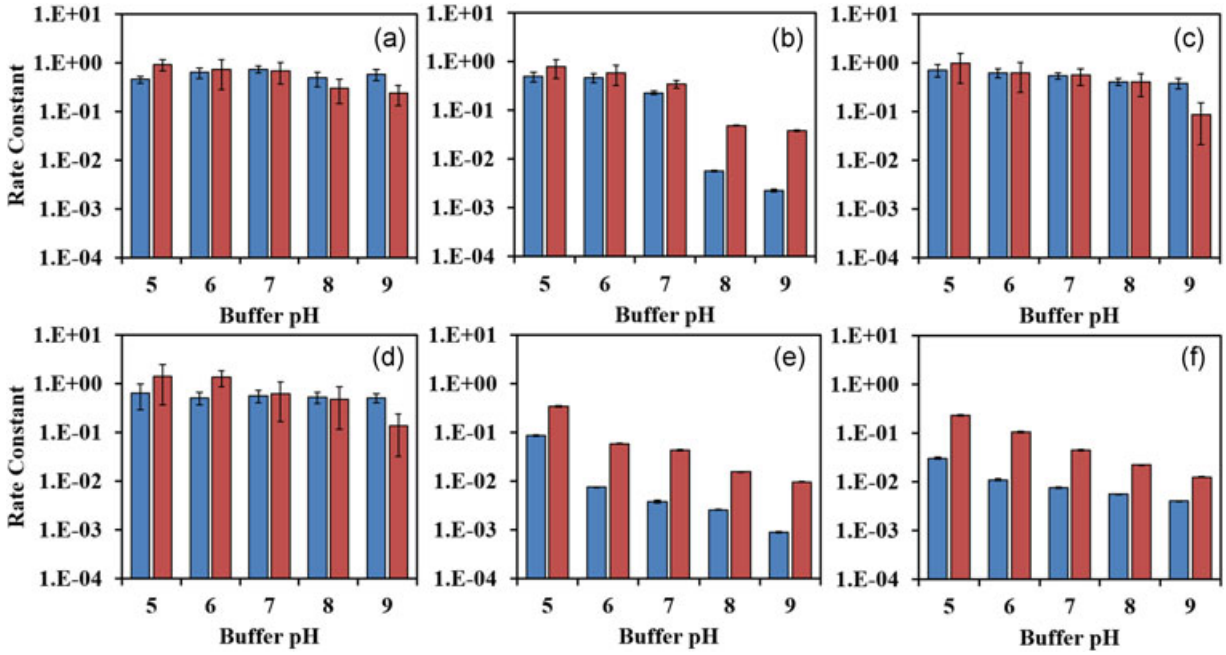

FIGURE 3 F–W model rate constants k_1 (blue) and k_2A_0 (red) fit from absorbance data for mAb A (a), mAb B (b), mAb C (c), mAb D (d), Fc A (e), and polyclonal antibody (f). mAb, monoclonal antibody [Color figure can be viewed at wileyonlinelibrary.com]

at pH 5, the maximum aggregation rate occurred within 10 min and the rate constants increased 10-fold compared with pH 6 (Figure 3e). This result is significant as we can dramatically reduce the time required for Fc A precipitation from 3 hr to 10 min simply by titrating the cell culture to pH 5. Similarly, the aggregation kinetics of the human polyclonal IgG also increased at lower pH. Using isoelectric focusing, the pI value for the human polyclonal antibody has been estimated to be between pH 5 and 7 (Szenczi, Kardos, Medgyesi, & Závodszky, 2006). The rate constants gradually increased at lower buffer pH, likely due to a larger majority of cationic antibodies within the polyclonal antibody population. This result validates our previous observations of lower polyclonal antibody precipitation yields and slower aggregation kinetics compared with mAb C (Swartz et al., 2018). This analysis suggests that the time required for precipitation of any target mAb with a pI value less than seven may be minimized to <10 min by simply titrating the cell culture to a lower pH.

Overall, lowering the buffer pH to 5 resulted in higher kinetics rates for all molecules. These results suggest that molecules with a net positive charge under more acidic solution conditions have a higher propensity for nanocage crosslinking. The higher degree of crosslinking is unlikely to be the result of improved mAb binding as the binding affinity of Z-domain decreases at more acidic pH (pH 5.0) compared with neutral pH (Tsukamoto, Watanabe, Ooishi, & Honda, 2014). Therefore, the increase in kinetics at lower pH is more likely due to other biophysical changes. Electrostatic interactions between the ELP and mAb may play a role in crosslinking. The Z-ELP fusion protein contains a small linker between the tri-helical Z-domain and cationic ELP (pI = 10.6, intrinsically disordered; Swartz et al., 2017). A negative net charge on the mAb may attract the positively charged ELP (at all solution pH 5–9) and sterically disrupt interaction with the Z-domain. In contrast, higher crosslinking efficiency may be obtained if the net ELP–mAb interaction is repulsive at solution pH less than the mAb pI value, as detected here.

The effects of solution pH on aggregation rates have been postulated for other protein systems. For the amyloid protein, α-synuclein, the aggregation rate increases as the solution pH is decreased from 8 to below the pI (pH~4) due to conformational changes that increased protein–protein interactions (Uversky, Li, & Fink, 2001). The aggregation kinetics of amyloid proteins were characterized by the F–W model and a similar result was obtained as in the current work: Nucleation rates (k_1) were significantly higher at a solution pH < protein pI (Morris and Finke, 2009). This provides an easily tunable parameter for minimizing the time required for aggregation using a simple pH shift.

3.3 | Elution buffer pH and mAb stability

After polymerizing into large aggregates, the mAb–nanocage complex remained insoluble until dissolution with a low-pH elution. To separate dissociated mAbs after elution in a low-pH buffer, the nanocage was selectively precipitated by adding 0.4 M ammonium sulfate and the eluted mAbs were collected in the supernatant after centrifugation. Previously, we demonstrated that citrate elution buffer was ideal for minimizing pH drift when resuspending at higher concentrations (Swartz et al., 2018). Consistent with the previous results, the critical solution pH to dissociate mAbs from the Z-domain was at pH < 4.0; an mAb recovery yield >90% was obtained at pH 3.50 and 3.75 for all molecules (Figure 4). Above pH 4.0, mAbs did not fully dissociate from the Z-domain, resulting in the coprecipitation of mAbs still bound within the crosslinked network. At pH 5,

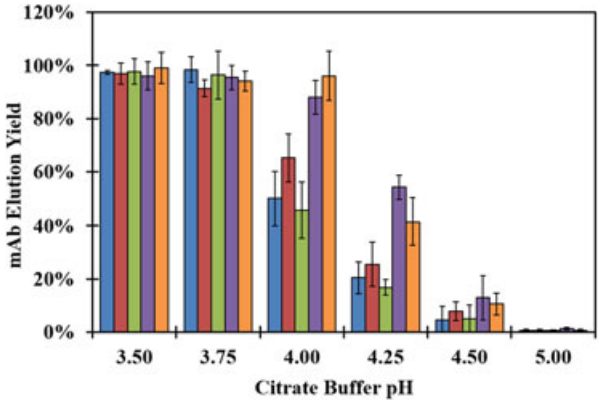

FIGURE 4 Effect of 50 mM sodium citrate buffer pH on mAb elution yield for mAb A (blue), mAb B (red), mAb C (green), mAb D (purple), and Fc A (orange). mAb, monoclonal antibody [Color figure can be viewed at wileyonlinelibrary.com]

minimal mAb (<1.5%) was detected in the supernatant, indicating that a solution pH of ≥5 was compatible for washing or precipitation. This result corroborates the aggregation kinetics investigation where all molecules rapidly aggregated into insoluble precipitates at pH 5.

Because some mAbs have been shown to aggregate at pH < 4 in the presence of salt (Arosio, Jaquet, Wu, & Morbidelli, 2012), the effect of elution pH and salt concentration on monomer content was further investigated in a 50 mM sodium citrate pH 3.5 buffer with 0.0–0.3 M ammonium sulfate concentration (Figure 5a). Samples were combined in a target buffer and mixed for 120 min at 23°C before titrating back to pH 5.5 for measurements by SEC. The titration to pH 5.5 was performed to mimic the procedure used with conventional Protein A chromatography, where the elution pool is titrated to pH > 5 after a viral inactivation to mitigate any potential detrimental impacts of low pH on mAb stability (Shukla, Hubbard, Tressel, Guhan, & Low, 2007). Although mAb C, mAb D, and Fc A were all stable at pH 3.5 and ammonium sulfate up to 0.3 M, mAb A and B were only stable in 50 mM sodium citrate pH 3.5 without added salt, and exhibited significant aggregation in the presence of 0.1 M ammonium sulfate.

To determine the optimal elution pH while providing maximum product recovery, mAb A and B monomer content was measured after an incubation of 120 min in citrate buffers pH 3.5–5.0 with 0.2 M ammonium sulfate, followed by a titration to pH 5.5 (Figure 5b). The monomer content greatly improved at pH 3.75 and was >98% at pH 4 and 5. Because pH 3.75 was sufficient for high elution yields (Figure 4), 50 mM citrate pH 3.75 and 0.2 M ammonium sulfate was selected for the precipitation and purification of mAb A and B from cell culture.

3.4 | Affinity precipitation from clarified cell culture harvests

After optimization of process conditions for each target protein, affinity precipitation was performed from clarified cell culture harvests according to the indicated procedures (Table 2). mAb A, C, and D were mixed with nanocages at a 3:1 Z:mAb molar ratio directly in cell culture (pH 7.0–7.5). Because of the slower aggregation kinetics, mAb B and Fc A were titrated to pH 5.0 using 1 M citric acid before precipitation with the nanocage. The pelleted mAb–nanocage

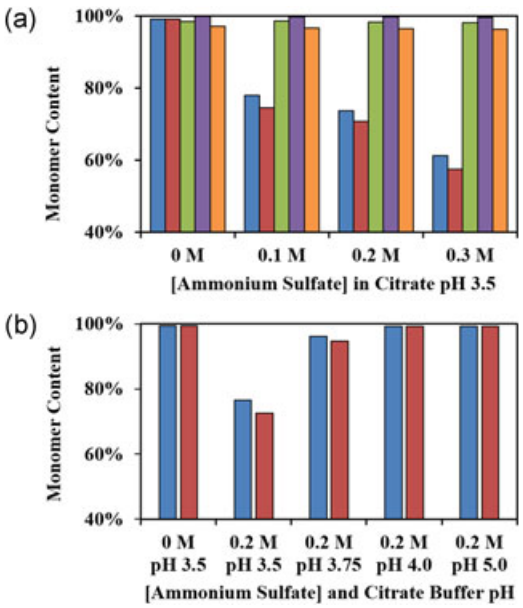

FIGURE 5 mAb elution stability. (a) Effect of ammonium sulfate concentration on mAb stability in 50 mM sodium citrate pH 3.5 for mAb A (blue), mAb B (red), mAb C (green), mAb D (purple), and Fc A (orange). (b) Effect of pH on mAb stability in 50 mM sodium citrate buffers with 0.2 M ammonium sulfate for mAb A (blue) and mAb B (red). mAb, monoclonal antibody [Color figure can be viewed at wileyonlinelibrary.com]

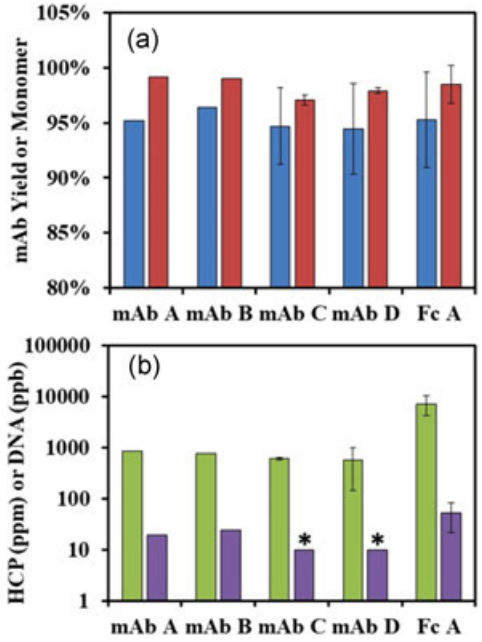

FIGURE 6 Characterization of mAb affinity precipitation from cell culture. (a) mAb elution yield (blue) or monomer content (red). (b) Elution impurity content for HCP (green) or DNA (purple). * indicates concentration less than detectable in the assay. HCP, host cell protein; mAb, monoclonal antibody [Color figure can be viewed at wileyonlinelibrary.com]

TABLE 3 Comparison of the average affinity precipitation performance for mAbs A–D with expected Protein A chromatography performance

Unit operation	mAb yield (%)	Monomer (%)	HCP (ppm)	DNA (ppb)	Nanocage yield (%)
Affinity precipitation	95.2 ± 1.4	98.3 ± 1.6	701 ± 218	<15.8 ± 11.1[a]	86.8 ± 4.6
Protein A chromatography[b]	>95	>95	200–3,000	100–1,000	n/a

Note. Average affinity precipitation values are reported with 95% confidence intervals. HCP, host cell protein; mAb, monoclonal antibody.
[a]<10 ppb for mAb C and D included in calculation.
[b]From Fahrner et al. (2001).

complex was washed with a series of three buffers. For mAbs A–D, the second wash buffer contained 0.05% (w/v) PS-80 to remove trace contaminants (Swartz et al., 2018), whereas PS-80 was excluded for Fc A because of protein stability concerns. mAb A and B were eluted with a 50 mM citrate buffer (pH 3.75), whereas other molecules were eluted with a 50 mM citrate buffer (pH 3.50) in threefold less volume to concentrate the target proteins. The nanocage was precipitated with 0.2–0.3 M ammonium sulfate and the mAbs were collected in the supernatant and titrated to pH 5.5. After recycling back into PBS, the nanocage was sterile filtered through a 0.2 μm membrane before reuse in additional purification cycles.

The mAb elution samples were characterized by the overall yield, % monomer, and HCP and DNA impurity content (Figure 6). The final product yields ranged from 94% to 97% and the monomer content exceeded 97% for all targets. The HCP and DNA clearance was consistent for mAbs A–D with < 1,000 ppm HCP (~3 log reduction) and <50 ppm DNA (4–5 log reduction; Supporting Information Figure S2). However, Fc A did not show such efficient HCP impurity clearance, with only 2 logs of reduction. One reason for this poor clearance could be because the second wash buffer did not contain PS-80, which has been shown to be beneficial for HCP clearance by reducing nonspecific interactions (Shukla & Hinckley, 2008). Further optimization of the wash buffer conditions could potentially improve on this result. Compared with Protein A chromatography, the average affinity precipitation performance of mAbs A–D fulfilled or exceeded all expectations for yield, monomer, and impurity content (Table 3). The average nanocage recovery for an affinity precipitation purification cycle was about 87% (Supporting Information Table S3). As discussed previously (Swartz et al., 2018), this low nanocage yield was likely due to losses to the container or sterile filter from operational constraints during the regeneration steps. Furthermore, the nanocage recovery may be improved by more efficient ELP precipitation with longer ELPs and higher ELP grafting density on the E2 nanocage. These results indicate that the proposed affinity precipitation process can consistently achieve high yield and impurity clearance for any target mAb with only minor optimization of the binding pH and elution stability profile.

4 | CONCLUSIONS

Affinity precipitation of mAbs using Z-ELP-E2 nanocages has been shown to be a promising alternative to Protein A chromatography because of the following three key features. (1) Spontaneous crosslinking allows for rapid affinity capture and precipitation at ambient temperature without added salt. (2) Irreversible insoluble precipitate formation allows for washing in most target buffer with pH ≥ 5 or extended storage of the mAb–nanocage complex. (3) Enlarged nanocage dimension minimizes the salt concentration required for precipitation after elution.

In this study, we challenged the nanocage affinity precipitation process using four industrial mAbs and one Fc fusion protein. For all target proteins, a 3:1 Z:mAb binding ratio was sufficient to precipitate >95% mAb in the solution mixture. mAb A, C, and D aggregated very quickly (<10 min), but mAb B (30 min) and more notably Fc A (3 hr) displayed slower kinetics in PBS buffer pH 7.2. Because of differences in the pI values for different targets, we hypothesized that the rate of crosslinking may depend on solution pH. An F–W kinetic model was applied to quantify aggregation rate constants representing initial multivalent binding (nucleation) and network formation into large precipitates (autocatalytic growth). We found that slow aggregation kinetics occurred at a solution pH close to or greater than the protein pI, and suspected that this may be due to attractive interactions between the cationic ELP and mAb that sterically decrease multivalent crosslinking efficiency. For mAb B and Fc A, fast aggregation (t_{max} < 10 min) was achieved at pH 5 and this finding was verified using cell culture titrated to pH 5. All molecules were eluted with >90% yield at pH < 4 and were stable in 50 mM citrate buffer pH 3.5 without added salt. mAb C, mAb D, and Fc A were stable in up to 0.3 M ammonium sulfate for 120 min, followed by titration to pH 5.5. mAb A and B demonstrated significant aggregation at pH 3.5 with salt, but were more stable at pH 3.75 after titration to pH 5.5.

The five molecules were purified from clarified cell culture using the indicated procedures and high mAb yield (95%) and monomer (>97%) were obtained. Nanocage affinity precipitation resulted in a clearance of 99.9% HCP and >99.99% DNA impurities from mAb A–D cultures. Fc A impurity clearance was not as efficient as the other mAbs, which may be due to the lack of PS-80 in the second wash buffer or due to stronger impurity-Fc A interactions compared with the other molecules. Affinity precipitation of mAbs A–D fulfilled or exceeded expectations of Protein A chromatography performance. Future work will focus on a more rigorous examination of nanocage regeneration and number of purification cycles, the use of filtration as a more scalable alternative to centrifugation, and the implementation of affinity precipitation in continuous processing.

ACKNOWLEDGMENTS

This work was supported by a grant from NSF (CBET1403724) and the GOALI Program Collaboration. We would like to thank BMS

Biologics Process Development (Devens, MA) for providing the mAb and for their technical and analytical support.

CONFLICTS OF INTEREST

The author declare that there is no conflicts of interest.

ORCID

Zheng Jian Li http://orcid.org/0000-0002-1941-4145
Wilfred Chen http://orcid.org/0000-0002-6386-6958

REFERENCES

Arosio, P., Jaquet, B., Wu, H., & Morbidelli, A. (2012). On the role of salt type and concentration on the stability behavior of a monoclonal antibody solution. *Biophysical Chemistry*, *168*, 19–27.

Bentea, L., Watzky, M. A., & Finke, R. G. (2017). Nucleation and growth curves across nature fit by the finke–watzky model of slow continuous nucleation and autocatalytic growth: Explicit formulas for the lag and growth times plus other key insights. *Journal of Physical Chemistry C*, *121*, 5302–5312.

Fahrner, R. L., Knudsen, H. L., Basey, C. D., Galan, W., Feuerhelm, D., Vanderlaan, M., & Blank, G. S. (2001). Industrial purification of pharmaceutical antibodies: Development, operation, and validation of chromatography processes. *Biotechnology and Genetic Engineering Reviews*, *18*(1), 301–327.

Flygare, S., Griffin, T., Larsson, P. O., & Mosbach, K. (1983). Affinity precipitation of dehydrogenases. *Analytical Biochemistry*, *133*, 409–416.

Gagnon, P. (2012). Technology trends in antibody purification. *Journal of Chromatography A*, *1221*, 57–70.

Hillbrig, F., & Freitag, R. (2003). Protein purification by affinity precipitation. *Journal of Chromatography B*, *848*(1), 40–47.

Hober, S., Nord, K., & Linhult, M. (2007). Protein A chromatography for antibody purification. *Journal of Chromatography B*, *848*, 40–47.

Jendeberg, L., Persson, B., Andersson, R., Karlsson, R., Uhlén, M., & Nilsson, B. (1995). Kinetic analysis of the interaction between Protein A domain variants and human Fc using plasmon resonance detection. *Journal of Molecular Recognition*, *8*(4), 270–278.

Low, D., O'Leary, R., & Pujar, N. S. (2007). Future of antibody purification. *Journal of Chromatography B*, *848*(1), 48–63.

Madan, B., Chaudhary, G., Cramer, S. M., & Chen, W. (2013). ELP-z and ELP-zz capturing scaffolds for the purification of immunoglobulins by affinity precipitation. *Journal of Biotechnology*, *163*(1), 10–16.

Meyer, D. E., & Chilkoti, A. (1999). Purification of recombinant proteins by fusion with thermally-responsive polypeptides. *Nature Biotechnology*, *17*(11), 4–1115.

Morris, A. M., & Finke, R. G. (2009). α-Synuclein aggregation variable temperature and variable pH kinetic data: A re-analysis using the Finke–Watzky 2-step model of nucleation and autocatalytic growth. *Biophysical Chemistry*, *140*, 9–15.

Morris, A. M., Watzky, M. A., Agar, J. N., & Finke, R. G. (2008). Fitting neurological protein aggregation kinetic data via a 2-step, Minimal/"Ockham's Razor" model: The Finke-Watzky mechanism of nucleation followed by autocatalytic surface growth. *Biochemistry*, *47*, 2413–2427.

Sheth, R. D., Jin, M., Bhut, B. V., Liu, J., Lee, J., Siegfried, R., … Cramer, S. M. (2014). Affinity precipitation of monoclonal antibody from industrial harvest feedstock using ELP-Z stimuli responsive biopolymers. *Biotechnology and Bioengineering*, *111*, 1595–1603.

Sheth, R. D., Madan, B., Chen, W., & Cramer, S. M. (2013). High throughput screening for the development of a monoclonal antibody affinity precipitation step using ELP-Z stimuli responsive biopolymers. *Biotechnology and Bioengineering*, *110*, 2664–2676.

Shukla, A. A., & Hinckley, P. (2008). Host cell protein clearance during Protein A chromatography: Development of an improved column wash step. *Biotechnology Progress*, *24*(5), 1115–1121.

Shukla, A. A., Hubbard, B., Tressel, T., Guhan, S., & Low, D. (2007). Downstream processing of monoclonal antibodies – Application of platform approaches. *Journal of Chromatography B*, *848*(1), 28–39.

Shukla, A. A., & Thömmes, J. (2010). Recent advances in large-scale production of monoclonal antibodies and related proteins. *Trends in Biotechnology*, *28*(5), 253–261.

Swartz, A. R., Sun, Q., & Chen, W. (2017). Ligand-induced crosslinking of Z-ELP-functionalized E2 protein nanoparticles for enhanced affinity precipitation of antibodies. *Biomacromolecules*, *18*(5), 1654–1659.

Swartz, A. R., Xu, X., Traylor, S. J., Li, Z. J., & Chen, W. (2018). One-step affinity capture and precipitation for improved purification of an industrial monoclonal antibody using Z-ELP functionalized nanocages. *Biotechnology and Bioengineering*, *115*(2), 423–432.

Szenczi, Á., Kardos, J., Medgyesi, G. A., & Závodszky, P. (2006). The effect of solvent environment on the conformation and stability of human polyclonal IgG in solution. *Biologicals*, *36*, 5–14.

Thommes, J., & Etzel, M. (2007). Alternatives to chromatographic separations. *Biotechnology Progress*, *23*, 42–45.

Tsukamoto, M., Watanabe, H., Ooishi, A., & Honda, S. (2014). Engineered Protein A ligands, derived from a histidine-scanning library, facilitate the affinity purification of IgG under mild acidic conditions. *Journal of Biological Engineering*, *8*, 15.

Uversky, V. N., Li, J., & Fink, A. L. (2001). Evidence for a partially folded intermedia in α-synuclein fibril formation. *The Journal of Biological Chemistry*, *276*, 10737–10744.

Watzky, M. A., Morris, A. M., Ross, E. D., & Finke, R. G. (2008). Fitting yeast and mammalian prion aggregation kinetic data with the Finke-Watzky two-step model of nucleation and autocatalytic growth. *Biochemistry*, *47*, 10790–10800.

SUPPORTING INFORMATION

Additional supporting information may be found online in the Supporting Information section at the end of the article.

How to cite this article: Swartz AR, Xu X, Traylor SJ, Li ZJ, Chen W. High-efficiency affinity precipitation of multiple industrial mAbs and Fc-fusion proteins from cell culture harvests using Z-ELP-E2 nanocages. *Biotechnology and Bioengineering*. 2018;115:2039–2047.
https://doi.org/10.1002/bit.26717